

Cosmic Shear from Scalar-Induced Gravitational Waves

Devdeep Sarkar¹, Paolo Serra¹, Asantha Cooray¹, Kiyotomo Ichiki², Daniel Baumann³

¹*Center for Cosmology, Department of Physics and Astronomy,
4129 Frederick Reines Hall, University of California, Irvine, CA 92697*

²*Research Center for the Early Universe, University of Tokyo,
7-3-1 Hongo, Bunkyo-ku, Tokyo 113-0033, Japan*

³*Department of Physics, Princeton University, Princeton, NJ 08544*

(Dated: October 29, 2018)

Weak gravitational lensing by foreground density perturbations generates a gradient mode in the shear of background images. In contrast, cosmological tensor perturbations induce a non-zero curl mode associated with image rotations. In this note, we study the lensing signatures of both primordial gravitational waves from inflation and second-order gravitational waves generated from the observed spectrum of primordial density fluctuations. We derive the curl mode for galaxy lensing surveys at redshifts of 1 to 3 and for lensing of the cosmic microwave background (CMB) at a redshift of 1100. We find that the curl mode angular power spectrum associated with secondary tensor modes for galaxy lensing surveys dominates over the corresponding signal generated by primary gravitational waves from inflation. However, both tensor contributions to the shear curl mode spectrum are below the projected noise levels of upcoming galaxy and CMB lensing surveys and therefore are unlikely to be detectable.

PACS numbers: 98.80.Es,95.85.Nv,98.35.Ce,98.70.Vc

I. INTRODUCTION

The weak lensing of background sources such as galaxies at redshifts of 1 to 3 and cosmic microwave background (CMB) fluctuations at a redshift of 1100 by foreground density perturbations is now well understood [1, 2, 3]. In addition to the lensing by density perturbations, metric tensor perturbations associated with gravitational waves also lens background images [4, 5]. While the lensing by gravitational waves was first considered to be negligible [4], the advent of high precision weak lensing surveys (both from the ground and from space) as well as the potential availability of high resolution and high sensitivity CMB anisotropy and polarization maps has renewed interest in the lensing by gravitational waves [6, 7].

An important source of cosmological gravitational waves are quantum fluctuations during the inflationary era. The weak lensing of background galaxy images [6] and CMB anisotropies [7] by these primordial tensor modes has previously been discussed in the literature. Even for the maximal inflationary gravitational wave amplitude consistent with current observations (corresponding to a tensor-to-scalar ratio, $r \lesssim 0.4$), the weak lensing effect on galaxy images is below the noise level even for a next-generation all-sky lensing survey and is therefore unlikely to be detectable [6]. For lensing of CMB anisotropies and polarization, the modifications imposed by foreground gravitational waves with a tensor-to-scalar ratio below 0.4 is again smaller than the cosmic variance for all-sky CMB anisotropy and polarization measurements [7].

While previous studies have concentrated on the lensing by first-order primordial gravitational waves, a secondary spectrum of gravitational waves is generated at

by second-order by the observed primordial density fluctuations [8]. These tensors produce a B-mode spectrum in the CMB polarization [9] with an equivalent amplitude that is about 10^{-6} in the (first-order) tensor-to-scalar ratio, after accounting for late-time reionization contribution to CMB polarization [10]. In the presence of residual polarized foregrounds and the confusion produced by weak lensing of CMB anisotropies by foreground density perturbations [11], such a signal is in practice unobservable. Furthermore, the present amplitude of secondary scalar-induced gravitational waves is below the projected sensitivity for future experiments like the Big Bang Observer (BBO) at the wavelengths corresponding to space-based direct detection experiments [12]. However, on larger scales secondary gravitational waves are continuously sourced by a non-linear scalar source term. As a consequence secondary gravitational waves have a non-trivial transfer function and the late-time spectrum is enhanced on cosmological length scales relative to the small scales accessible to direct detection experiments [13]. In particular, on comoving scales of order the horizon size at matter-radiation equality ($\sim k_{\text{eq}}^{-1}$) second-order gravitational wave does not redshift and their amplitude stays constant. This is in contrast to (first-order) primordial gravitational waves that redshift on all scales. This effect leads to a peak of the secondary gravitational wave spectrum on large scales (around k_{eq}) which could potentially be probed with weak lensing of galaxies at redshifts of 1 to 3 (see Figures 1 and 3 in Ref. [13]).

The identification of lensing by gravitational waves is aided by the fact that the lensing deformation associated with tensors leads to a curl mode in cosmic shear [5, 14]. Foreground density perturbations do not generate a curl mode in cosmic shear, except at second-order and at small angular scales due to effects such as lens-lens coupling [15]. The situation is analogous to the curl (B)

and the gradient (E) modes of CMB polarization, where only gravitational waves source the curl or B-mode [9].

The paper is organized as follows. In Section II we review theoretical aspects of lensing by foreground gravitational waves. Computing the lensing signals requires input power spectra and transfer functions for both primordial tensors and the secondary tensors sourced by primordial density perturbations. We provide these results in Section III. In Section IV we present our results on the shear curl mode angular power spectrum. We conclude in Section V.

When presenting numerical calculations, we will assume a flat- Λ CDM cosmology with $\Omega_m = 0.3$ and $h = 0.7$.

II. WEAK LENSING BY GRAVITY WAVES

In weak gravitational lensing, density perturbations only lead to image distortions involving amplification (or convergence) κ . However, the lensing by gravitational waves leads to both convergence and rotation ω , involving the anti-symmetric part of the weak lensing deformation matrix [15]

$$\mathbf{A} = \begin{pmatrix} 1 - \kappa - \gamma_1 & -\gamma_2 - \omega \\ -\gamma_2 + \omega & 1 - \kappa + \gamma_1 \end{pmatrix}, \quad (1)$$

where all components are functions of the position on the sky $\hat{\mathbf{n}}$ and γ_i are two shear components [3]. $(\mathbf{A})_{ij} \equiv A_{ij}$ maps between the source plane (S) and the image plane (I) such that $\delta x_i^S = A_{ij} \delta x_j^I$.

For lensing by foreground gravitational waves, the geodesic equation is [6]

$$\ddot{\mathbf{r}} = \frac{1}{2} \left(\dot{\mathbf{r}} \cdot \dot{\mathbf{H}} \cdot \dot{\mathbf{r}} \right) \dot{\mathbf{r}} - (\mathbf{1} + \mathbf{H})^{-1} \cdot \left[\dot{\mathbf{r}} \cdot \frac{d}{d\eta} \mathbf{H} - \frac{1}{2} \nabla_H (\dot{\mathbf{r}} \cdot \mathbf{H} \cdot \dot{\mathbf{r}}) \right], \quad (2)$$

where, to simplify notation, the explicit dependence on η in each of these terms has been suppressed. Here, over-dots represent derivatives with respect to conformal time and $(\mathbf{H})_{ij} \equiv h_{ij}$ is the transverse ($\nabla \cdot \mathbf{H} = 0$) and traceless ($\text{Tr} \mathbf{H} = 0$) tensor metric perturbation representing gravitational waves. The operator ∇_H denotes the gradient applied only to the metric perturbation \mathbf{H} ; when not subscripted with H , the gradient should be interpreted as applying to all terms, including the line-of-sight directional vector $\hat{\mathbf{n}}$. The solution to the above equation, $\mathbf{r}(\hat{\mathbf{n}}, \eta)$, is discussed in Refs. [6, 7].

Using the transverse displacement associated with a perturbed photon trajectory, the angular deflection projected onto the sky is $\vec{\Delta} = [\mathbf{r} - (\hat{\mathbf{n}} \cdot \mathbf{r}) \hat{\mathbf{n}}] / (\eta_0 - \eta)$. This can be related to the convergence κ and the rotation ω in the weak lensing deformation matrix [5]

$$\kappa \equiv -\frac{\Delta_a{}^a}{2}, \quad \text{and} \quad \omega \equiv \frac{(\Delta_a \epsilon^{ab})_{:b}}{2}, \quad (3)$$

where the colons denote covariant derivatives with respect to the perturbed FRW metric [5].

A simple argument explains why gravitational waves h_{ij} lead to an image rotation. If we take the line-of-sight to be in the $\hat{\mathbf{z}}$ -direction, then $\omega \propto \epsilon_{kl} \partial_k h_{zl}$. If the gravitational wave propagates in the $\hat{\mathbf{y}}$ -direction, then $\omega \propto \partial_y h_{zx}$ and the deflection is in the $\hat{\mathbf{x}}$ -direction with $\delta\theta_x \propto h_{zx}$.

Integrating over all deflections along the line-of-sight to a background image at η_S , we can write the rotational component as [5]

$$\begin{aligned} \omega(\hat{\mathbf{n}}) &\equiv -\frac{1}{2} \hat{\mathbf{n}} \cdot (\nabla \times \mathbf{r}(\hat{\mathbf{n}}, \eta_S)) \\ &= \frac{1}{2} \int_{\eta_S}^{\eta_0} d\eta' [\hat{\mathbf{n}} \cdot (\nabla \times \mathbf{H}) \cdot \hat{\mathbf{n}}]. \end{aligned} \quad (4)$$

Assuming isotropy, the three-dimensional spatial power spectrum of initial metric fluctuations related to a stochastic background of gravitational waves is

$$\langle h_{(i)}(\mathbf{k}) h_{(j)}^*(\mathbf{k}') \rangle = (2\pi)^3 P_t(k) \delta_{ij} \delta^{(3)}(\mathbf{k} - \mathbf{k}'), \quad (5)$$

where the two linear-polarization states of the gravitational wave are denoted by $(i), (j) = \times, +$. Taking the spherical-harmonic moments of Eq. (4) and using $(\nabla \times \mathbf{H})_{il} = \epsilon_{ijk} \partial_j h_{kl}$, the angular power spectrum of the rotational component becomes [6, 7]

$$\begin{aligned} C_l^{\omega\omega} &= \frac{1}{2l+1} \sum_{m=-l}^l \langle |\omega_{lm}|^2 \rangle \\ &= \frac{2}{\pi} \int k^2 dk P_t(k) |T_l^\omega(k, \eta_S)|^2, \end{aligned} \quad (6)$$

where

$$\begin{aligned} T_l^\omega(k, \eta_S) &= \\ &= \sqrt{\frac{(l+2)!}{(l-2)!}} \int_{\eta_S}^{\eta_0} k d\eta' T_t(k, \eta') \frac{j_l(x)}{x^2} \Big|_{x=k(\eta_0-\eta')} \end{aligned} \quad (7)$$

Here $T_t(k, \eta)$ represents the transfer function of tensor perturbations.

III. SECONDARY TENSOR SPECTRUM

The derivation of the cosmic shear curl modes from a spectrum of tensor fluctuations has so far made no reference to the form of the underlying power spectrum $P_t(k)$ and the transfer function $T_t(k, \eta)$. The previous results are therefore applicable to different sources for cosmological gravitational waves. In standard inflationary models, the primordial tensor fluctuation spectrum is predicted to be

$$P_t(k) = A_t k^{n_t-3}. \quad (8)$$

Inflationary models generally predict that $n_t \sim 0$ while the ratio of tensor-to-scalar amplitudes, $r = A_t/A_s$, is

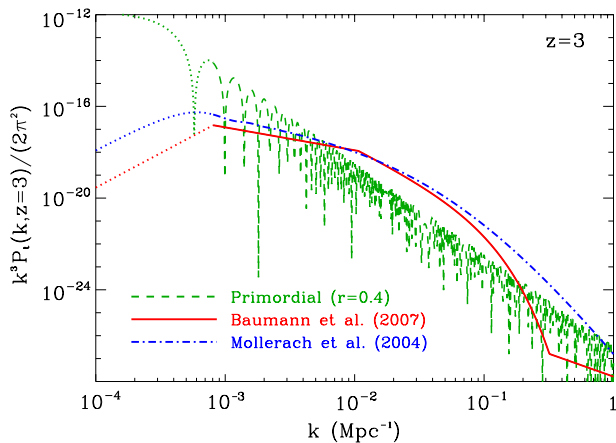


FIG. 1: The power spectrum of primordial (dashed line) and secondary gravitational waves at $z = 3$. For the secondary spectrum, we show results from two calculations in the literature: the solid line is from Baumann et al. [13] and the dot-dashed line from Mollerach et al. [10]. The dotted part of the spectra corresponds to superhorizon scales at $z = 3$.

now constrained to be $\lesssim 0.4$ [16]. We will use this upper limit when calculating the inflationary gravitational wave contribution to shear curl modes. In addition to the primordial power spectrum, we also require the transfer function $T_t(k, \eta)$. This is obtained as a solution to the wave equation for primordial gravitational waves

$$\ddot{\mathbf{H}} - \nabla^2 \mathbf{H} + 2\frac{\dot{a}}{a}\mathbf{H} = 16\pi G a^2 \mathbf{P}, \quad (9)$$

where \mathbf{P} is the tensor part of the anisotropic stress, say due to neutrinos [17]. The term on the right hand side acts as a damping term for the evolution of gravitational waves and is important for modes that enter the horizon before matter-radiation equality, with a smaller correction for modes entering the horizon after matter-radiation equality. Ignoring this small correction, we take the transfer function for the primordial gravitational wave spectrum as $T_t(k, \eta) = 3j_1(k\eta)/(k\eta)$.

We now consider the spectrum and transfer function for cosmological gravitational waves which are created at second-order by the observed primordial density perturbations [8]. We make use of two calculations in the literature for the spectrum of secondary gravitational waves. Using results from Mollerach et al. [10], the secondary tensor power spectrum is given by

$$P_t^{\text{Mol}}(k) = \frac{12\pi^2}{25} C \Delta_{\mathcal{R}}^4(k_0) \frac{1}{k^3} \frac{k_*}{k} W(k/k_*) \left(\frac{k_*}{k_0}\right)^{2(n_s-1)}, \quad (10)$$

with $k_* = \Omega_m h^2 \text{Mpc}^{-1}$ and the coefficient $C(n_s) = 0.062$ when $n_s = 1$. The function $W(x)$ is well fitted by $W(x) = (1 + 7x + 5x^2)^{-3}$. The normalization of the scalar spectrum is taken to be $\Delta_{\mathcal{R}}^2(k_0 = 0.002 \text{Mpc}^{-1}) = 2.4 \times 10^{-9}$ [16] and to simplify the calculation we assume a spectral index for density perturbations with $n_s \sim 1$. Our results and conclusions are insensitive to assuming $n_s \sim 0.96$,

more consistent with recent WMAP results [16]. The transfer function associated with this secondary gravitational wave spectrum is

$$T_t^{\text{Mol}}(k, \eta) = \left(1 - \frac{3j_1(k\eta)}{k\eta}\right) g_\infty^2, \quad (11)$$

where g_∞ is the growth-suppression factor in the limit $z \rightarrow \infty$ [18].

The Mollerach et al. [10] calculation of secondary tensor fluctuations was recently extended by Baumann et al. [13] by accounting for the evolution over all wavenumbers during both radiation and matter domination. The analytical result for the scalar-induced gravitational wave power spectrum is [13]

$$P_t^{\text{Bau}}(k) = 2\pi^2 \left(\frac{4}{9}\right)^2 \Delta_{\mathcal{R}}^4(k_0) k^{-3} \left(\frac{k}{k_0}\right)^{2(n_s-1)} \times \begin{cases} \frac{k_{\text{eq}}}{k} & \text{if } k < k_{\text{eq}} \\ 1 & \text{if } k > k_{\text{eq}} \end{cases} \quad (12)$$

while the corresponding transfer function is

$$T_t^{\text{Bau}}(k, \eta) = \begin{cases} 1 & \text{if } k < k_{\text{eq}} \\ \left(\frac{k}{k_{\text{eq}}}\right)^{-\gamma(k)} & \text{if } k_{\text{eq}} < k < k_c(\eta) \\ \frac{a_{\text{eq}}}{a(\eta)} \frac{k_{\text{eq}}}{k} & \text{if } k > k_c(\eta) \end{cases} \quad (13)$$

where

$$k_c(\eta) = \left[\frac{a(\eta)}{a_{\text{eq}}}\right]^{1/(\gamma(k)-1)} k_{\text{eq}}. \quad (14)$$

Here, $k_{\text{eq}} = 0.073 \Omega_m h^2 \text{Mpc}^{-1}$ corresponds to the comoving horizon scale at matter-radiation equality. $\gamma(k)$ is a weakly k -dependent function which we fit by comparison to numerical calculations of the tensor power spectrum in Baumann et al. [13]. In practice, we use a smooth interpolation between k_{eq} and $k_c(\eta)$. For low z we find $\gamma(k_{\text{eq}}) = 1.5$ and $\gamma(k_c) = 3$. The analytical result presented here was found to be in agreement with full numerical result at the 10% level and is adequate for the purposes of this calculation.

IV. RESULTS AND DISCUSSION

In Figure 1, we give a comparison between the primordial gravitational wave spectrum with a tensor-to-scalar ratio of 0.4 and the secondary gravitational wave spectrum at $z = 3$. We show results from both Mollerach et al. [10] and Baumann et al. [13] for the second-order tensor spectrum. They agree at the percent level when $k < k_{\text{eq}} (= 0.0107 \text{Mpc}^{-1})$ and at high redshifts. For smaller scales, $k > k_{\text{eq}}$, and at low redshifts, due to differences in the treatment of the evolution of the tensor modes captured in the transfer function, the two calculations predict spectra that differ by more than a few

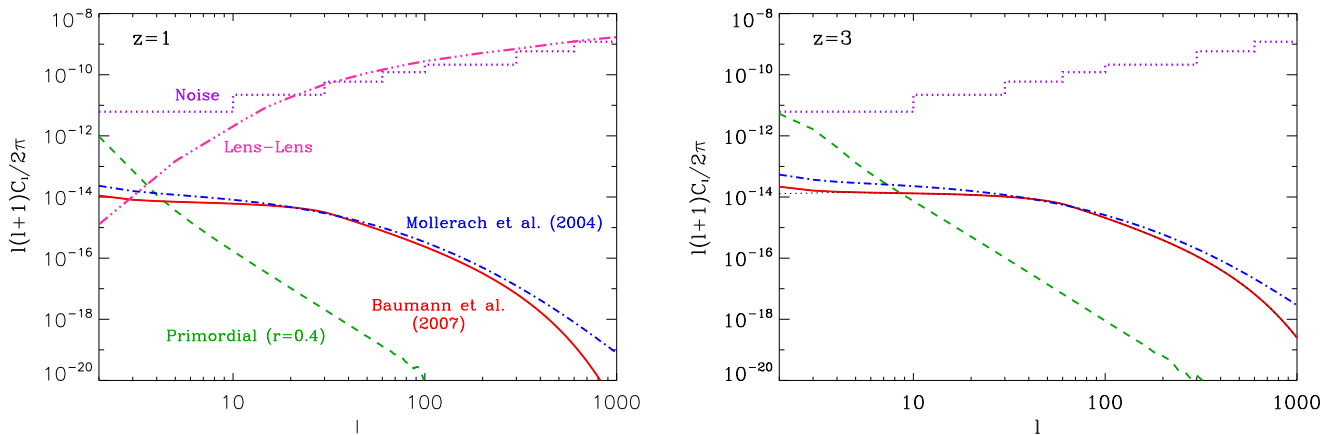


FIG. 2: The angular power spectra of the cosmic shear curl mode at $z = 1$ (left panel) and at $z = 3$ (right panel). The dotted line is the noise associated with a measurement of the shear curl mode power spectrum (see text for details). While the curl mode power spectrum is below the noise, the secondary gravitational waves produce a larger signal than the primordial tensor modes when $r < 0.4$. For reference, the double dot-dashed line on the left-panel shows the angular power spectrum of secondary shear curl modes generated by the coupling of two lenses (lens-lens coupling) along the line-of-sight to background sources at $z = 1$ [15].

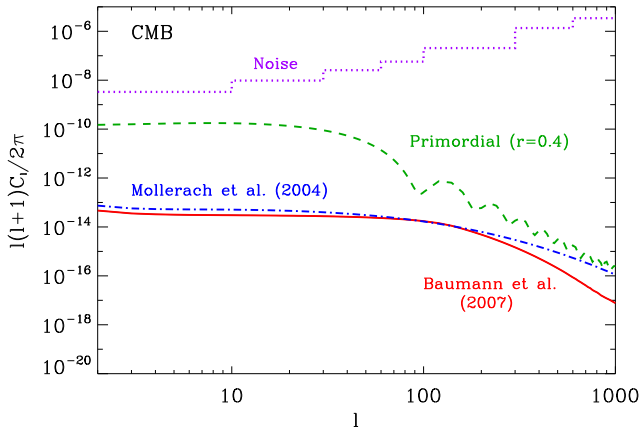


FIG. 3: The angular power spectrum of the curl mode at $z = 1100$ for lensing of CMB anisotropies by foreground gravitational waves. The dotted line shows the expected noise from a cosmic-variance limited reconstruction of the curl mode following Cooray et al. [14] using E- and B-mode CMB polarization maps. For CMB lensing, the primordial tensor modes dominate when $r \gtrsim 10^{-6}$.

percent. Baumann et al. [13] captures the correct transfer function for small scale gravitational waves.

In Figure 2, we show the weak lensing curl mode angular power spectrum for sources out to $z = 1$ and at $z = 3$. The dotted line in Fig. 2 shows the expected binned noise from an all-sky experiment similar to the one discussed in Dodelson et al. [6]. For weak lensing

shear, the binned noise is

$$\Delta C_l = \sqrt{\frac{2}{(2l+1)\Delta_l f_{\text{sky}} N_{\text{gal}}} \langle \gamma^2 \rangle}, \quad (15)$$

and we take $\langle \gamma \rangle$, the intrinsic ellipticity, to be 0.3 and $N_{\text{gal}} = 1.5 \times 10^{10}$ or roughly 100 galaxies per square-arcminute. The plotted noise power spectrum in Fig. 2 assumes varying bin sizes, Δ_l , but as shown there, even with wide bins in the multipole space, the detection of secondary tensor modes with the curl mode of cosmic shear remains challenging.

Even if we there were a technique to improve on the measurement noise of lensing surveys, the signal from secondary tensors will be heavily confused with another signal in the shear curl mode associated with the coupling of two lenses along the line-of-sight (lens-lens coupling; [15]). We show the resulting angular power spectrum out to $z = 1$ in the left panel of Fig. 2 with a double dot-dashed line. This signal peaks at small angular scales as it is generated by non-linear density perturbations. At multipoles of 10 to 100 where the secondary tensor signal is interesting the lens-lens coupling corrections to the rms of the curl mode is larger by a factor of 10 to 100.

While the signal is below the measurement noise and is confused with the lens-lens coupling signal in the curl modes of shear, the secondary tensor modes produce a larger curl mode at $\ell \sim 100$ than the primordial tensor modes from inflation with $r \lesssim 0.4$. Thus, we find that at large angular scales the curl modes of cosmic shear will be dominated by secondary gravitational waves and not the primordial signal from inflation. This is consistent with results in Baumann et al. [13] which show that at cosmologically interesting wavenumbers with $k \sim 10^{-3} \text{ Mpc}^{-1}$

to 0.1 Mpc^{-1} , the secondary spectrum dominates over the primordial spectrum at low redshifts. While such modes are not probed by a direct detection experiment such as the BBO, such modes are in the range that is in principle detectable with cosmic shear. Unfortunately, the amplitude is below what can be achieved with galaxy lensing surveys, even considering optimistic galaxy statistics and shear noise.

Finally, in Fig. 3, we plot C_l of cosmic shear for $z = 1100$ related to lensing of CMB anisotropies by foreground tensors [7]. The noise plotted here comes from a cosmic variance-limited reconstruction of the shear curl mode with a combination of E- and B-mode polarization maps [14, 19]. For both primordial gravitational waves and the secondary gravitational waves, a detection is unlikely to be achieved. In the case of the CMB, unlike galaxy lensing at low redshifts, the primordial tensors dominate the curl mode (for $r \gtrsim 10^{-6}$) since one is probing out to a high redshift where primordial modes are not significantly damped due to subsequent evolution.

V. CONCLUSION

At second-order in perturbation theory the measured spectrum of primordial density fluctuations generates a

secondary gravitational wave signal. In this paper, we computed the weak lensing signatures of these secondary tensor modes. We considered the use of the cosmic shear curl mode, or analogously the rotational component, as a diagnostic of these tensor modes since density perturbations at first-order do not generate a curl mode. We presented results both for galaxy lensing surveys at redshifts of 1 to 3 and lensing of cosmic microwave background (CMB) fluctuations at a redshift of 1100. At low redshifts, the signal associated with secondary tensor modes is larger than the shear curl mode from primary gravitational waves generated by inflation with a tensor-to-scalar ratio less than 0.4. However, we find that the expected shear curl mode spectrum from both primordial and secondary gravitational waves is very small and unlikely to be detectable with upcoming galaxy and CMB lensing surveys.

Acknowledgments

This work was supported by NSF CAREER AST-0645427 at UC Irvine. KI is supported by a Grant-in-Aid for the Japan Society for the Promotion of Science. DB thanks the Perimeter Institute for hospitality during completion of this work.

-
- [1] See, e.g., U. Seljak and M. Zaldarriaga, *Phys. Rev. Lett.* **82**, 2636 (1999); *Phys. Rev. D* **60**, 043504 (1999); M. Zaldarriaga and U. Seljak, *Phys. Rev. D* **59**, 123507 (1999); W. Hu, *Phys. Rev. D* **64**, 083005 (2001); W. Hu, *Phys. Rev. D* **62**, 043007 (2000); M. Zaldarriaga and U. Seljak, *Phys. Rev. D* **58**, 023003 (1998).
 - [2] A. Lewis and A. Challinor, arXiv:astro-ph/0601594.
 - [3] R. D. Blandford et al., *Mon. Not. Roy. Astron. Soc.* **251**, 600 (1991); J. Miralda-Escudé, *Astrophys. J.* **380**, 1 (1991); N. Kaiser, *Astrophys. J.* **388**, 277 (1992); M. Bartelmann and P. Schneider, *Astron. Astrophys.* **259**, 413 (1992).
 - [4] N. Kaiser and A. H. Jaffe, *Astrophys. J.* **484**, 545 (1997).
 - [5] A. Stebbins, arXiv:astro-ph/9609149.
 - [6] S. Dodelson, E. Rozo and A. Stebbins, *Phys. Rev. Lett.* **91**, 021301 (2003).
 - [7] C. Li and A. Cooray, *Phys. Rev. D* **74**, 023521 (2006).
 - [8] S. Matarrese, O. Pantano and D. Saez, *Phys. Rev. D* **47**, 1311 (1993); S. Matarrese, O. Pantano and D. Saez, *Phys. Rev. Lett.* **72**, 320 (1994); S. Matarrese, S. Mollerach and M. Bruni, *Phys. Rev. D* **58**, 043504 (1998); H. Noh and J. c. Hwang, *Phys. Rev. D* **69**, 104011 (2004); C. Carbone and S. Matarrese, *Phys. Rev. D* **71**, 043508 (2005); K. Nakamura, *Prog. Theor. Phys.* **117**, 17 (2007).
 - [9] M. Kamionkowski, A. Kosowsky, and A. Stebbins, *Phys. Rev. Lett.* **78**, 2058 (1997); U. Seljak and M. Zaldarriaga, *Phys. Rev. Lett.* **78**, 2054 (1997).
 - [10] S. Mollerach, D. Harari and S. Matarrese, *Phys. Rev. D* **69**, 063002 (2004).
 - [11] M. Kesden, A. Cooray, and M. Kamionkowski, *Phys. Rev. Lett.* **89**, 011304 (2002); L. Knox and Y.-S. Song, *Phys. Rev. Lett.* **89**, 011303 (2002); U. Seljak and C. Hirata, *Phys. Rev. D* **69**, 043005 (2004).
 - [12] K. N. Ananda, C. Clarkson and D. Wands, *Phys. Rev. D* **75**, 123518 (2007).
 - [13] D. Baumann, P. J. Steinhardt, K. Takahashi and K. Ichiki, *Phys. Rev. D* **76**, 084019 (2007).
 - [14] A. Cooray, M. Kamionkowski and R. R. Caldwell, *Phys. Rev. D* **71**, 123527 (2005).
 - [15] A. Cooray and W. Hu, *Astrophys. J.* **574**, 19 (2002); C. M. Hirata and U. Seljak, *Phys. Rev. D* **68**, 083002 (2003).
 - [16] E. Komatsu *et al.*, arXiv:0803.0547 [astro-ph]; J. Dunkley *et al.* [WMAP Collaboration], arXiv:0803.0586 [astro-ph].
 - [17] J. R. Pritchard and M. Kamionkowski, *Annals Phys.* **318**, 2 (2005).
 - [18] S. M. Carroll, W. H. Press and E. L. Turner, *Ann. Rev. Astron. Astrophys.* **30**, 499 (1992).
 - [19] T. Okamoto and W. Hu, *Phys. Rev. D* **67**, 083002 (2003).